

PAPER

[View Article Online](#)
[View Journal](#) | [View Issue](#)Cite this: *RSC Sustainability*, 2024, 2, 1979Received 3rd January 2024
Accepted 27th April 2024

DOI: 10.1039/d4su00002a

rsc.li/rscsusOne step conversion of bio-based magnolol into low k materials at high frequency†

Zhuoyi Yang, Jing Sun* and Qiang Fang *

A facile one-pot conversion of a bio-based magnolol gave a functional monomer with curable benzocyclobutene groups, which was then thermally polymerized to form a cross-linked resin, displaying a very low dielectric loss of 1.0×10^{-3} at a frequency of 10 GHz and a dielectric constant of 2.78, as well as exhibiting good dimensional stability with a CTE of 46 ppm °C⁻¹. These results indicate that the bio-based monomer has potential application as an encapsulation material used in the microelectronics industry.

Sustainability spotlight

In recent years, with the continuous reduction of traditional fossil energy reserves and the intensification of environmental pollution, clean biomass energy has entered the public's view. Increasing the commodity value added of biomass energy to replace non-renewable petroleum-based feedstocks can reduce greenhouse gas emissions and increase the share of renewable energy in the global energy mix. Aromatic biomass compounds always have apparent advantages when converted to functional materials because they have similar robust and rigid structures to the petrochemical aromatic monomers. Therefore, we use magnolol extracted from *Magnolia officinalis* as a raw material and convert it into a post-curable monomer through a one-step reaction, and the cured material has properties comparable to those of commercial products. Our work follows the principles of the UN sustainable development goals: affordable and clean energy (SDG 6), industry, innovation, and infrastructure (SDG 9), climate action (SDG 13).

Introduction

Among various natural products, magnolol is a very interesting compound. It contains two modified active groups including two allyl groups and two phenol units. Thus, this bio-based compound is an ideal starting material for the preparation of polymers, while most of the investigations focus on its pharmacological effects and its application as a fine chemical.^{1–5} There are a few reports regarding polymers based on magnolol.^{6–10} Therefore, investigation on the synthesis and properties of polymers based on magnolol is very desirable.

In recent years, much attention has been paid to organic materials with a low dielectric constant (D_k) and dielectric loss (D_f) at high frequencies of more than 5 GHz because of their broad application as encapsulation resins in the microelectronics industry, especially as basis materials in the new generation of communication.^{11–17} From the perspective of application, a satisfactory low dielectric material should possess not only a low dielectric constant of less than 2.80 and low dielectric loss of lower than 5.0×10^{-3} at a frequency of

higher than 5 GHz, but also display a low coefficient of thermal expansion (CTE)¹⁸ and good hydrophobicity.¹⁹ Thus, much effort has been made, and a lot of low dielectric materials have been explored and developed. Some examples include LCP,^{20–22} modified epoxies using active esters as curing agents^{23–27} and fluoro-containing polymers.^{28–31} However, there are a few species suitable for application in communication at high speed and high frequency. On the other hand, although commercial PTFE and its derivatives³² have been used in the electronics and microelectronics industries for many years, their processability and poor thermostability block their use. Hence, it is still necessary to develop suitable low dielectric materials.

It is noted that benzocyclobutene (BCB)-based polymers display good comprehensive properties including high thermostability,³³ good dielectric properties,¹⁹ good film-forming ability and bonding strength on substrates.^{11,19,34} Therefore, study of organic materials containing BCB groups would be a convenient way for exploring new low dielectric materials with good properties.^{15,30,35} Based on the ease of conversion of magnolol into the functional precursors of polymers, we have designed and synthesized a magnolol-based monomer with benzocyclobutene groups. This monomer (**M1**) is easily prepared by a one-step reaction in a moderate yield. The cured resin based on this exhibits a D_k of 2.78 and a very low D_f of 1.0×10^{-3} at a frequency of 10 GHz. In particular, the cured resin also exhibits good dimensional stability with a CTE of

Key Laboratory of Fluorine and Nitrogen Chemistry and Advanced Materials, Center for Excellence in Molecular Synthesis, Shanghai Institute of Organic Chemistry, University of Chinese Academy of Sciences, Chinese Academy of Sciences, 345 Lingling Road, Shanghai 200032, P. R. China. E-mail: qiangfang@sioc.ac.cn; sunjing@sioc.ac.cn; Fax: +86 21 5492 5337

† Electronic supplementary information (ESI) available: ¹³C NMR spectrum of **M1** as mentioned in the text (PDF). See DOI: <https://doi.org/10.1039/d4su00002a>

46 ppm °C⁻¹ and low water absorption of 0.5% even when immersed in boiling water for 96 h. These data imply that bio-based magnolol is an alternative resource for the preparation of electronic materials used in high technology fields. Here, we report the details.

Experimental section

Materials

Magnolol was purchased from Shanghai Defai Chemical Technology Co. Ltd. 4-Bromobenzocyclobutene was purchased from Chemtarget Technologies Co. Innocent (Beijing) Technology Co. Ligand L was purchased from Shanghai Haohong Biomedical Technology Co., Ltd. All solvents were used as received unless stated elsewhere.

Measurements

¹H NMR, ¹³C NMR, and ¹⁹F NMR spectra were collected on an AVANCE 500 spectrometer with CDCl₃ as the solvent. Elemental analysis (EA) was carried out using an Elementar VARIO ELIII apparatus. High-resolution mass spectrometry (HRMS) was performed using a Waters Premier GC-TOF MS instrument. Fourier transform-infrared (FT-IR) spectra were measured *via* a Thermo Scientific Nicolet spectrometer with KBr pellets in air. Differential scanning calorimetry (DSC) traces were obtained with a TA instrument (DSC Q200) at a heating rate of 10 °C min⁻¹ under a nitrogen flow. Thermogravimetric analysis (TGA) curves were recorded on a TG 209F1 apparatus in nitrogen with a heating rate of 10 °C min⁻¹. Dynamic mechanical analysis (DMA) was carried out on a DMA Q800 instrument in nitrogen with a heating rate of 5 °C min⁻¹. Thermal mechanical analysis (TMA) was performed on a TA Q400 instrument in nitrogen with a heating rate of 5 °C min⁻¹. The dielectric constant (*D_k*) and dielectric loss (*D_f*) were determined on a Keysight n5227A vector network analyzer with a split post-dielectric resonator at a frequency of 10 GHz.

Synthesis of 1

A mixture of magnolol (5.33 g, 20 mmol), 4-bromobenzocyclobutene (10 mL, 60 mmol), cuprous iodide (400 mg, 2 mmol), ligand L (672 mg, 2.4 mmol), cesium carbonate (13.04 g, 40 mmol), sodium L-ascorbate (1.58 g, 8.0 mmol), and dioxane (20.0 mL) was stirred at a refluxing temperature under an atmosphere of N₂ for 48 h, then cooled to room temperature and filtered. The filtrate was concentrated under reduced pressure. The obtained crude product was purified by column chromatography using *n*-hexane as the eluent. Pure **M1** was obtained as a white solid in a yield of 65%. ¹H NMR (500 MHz, CDCl₃) δ 7.21 (s, 1H), 7.03 (d, *J* = 6.8 Hz, 1H), 6.87 (d, *J* = 7.9 Hz, 1H), 6.79 (d, *J* = 8.3 Hz, 1H), 6.70 (d, *J* = 7.6 Hz, 1H), 6.57 (s, 1H), 6.07 ~ 5.82 (m, 1H), 5.16 ~ 4.93 (m, 2H), 3.36 (d, *J* = 6.4 Hz, 2H), 3.14–2.94 (m, 4H). ¹³C NMR (126 MHz, CDCl₃) δ 159.30, 156.92, 153.48, 146.04, 139.30, 137.36, 133.98, 131.84, 129.41, 128.52, 123.21, 118.24, 117.96, 115.59, 113.82, 77.16, 76.91, 76.65, 39.34, 28.81, 28.68. HRMS-EI (*m/z*): calcd for C₃₄H₃₀O₂,

470.2240, found, 470.2237. Anal. calcd for C₃₄H₃₀O₂: C, 86.78; H, 6.43. Found: C, 86.75; H, 6.47.

Preparation of the cured resin sheets for the measurement

A flat-bottomed glass tube with **M1** (1.20 g) was put into a quartz tube furnace under an atmosphere of argon, and the furnace was allowed to heat to 80 °C and maintained at the temperature for about 1 h. The furnace was then heated to 180 °C, and maintained at 180 °C, 200 °C, 220 °C and 240 °C for 2 h, respectively. A fully cured **M1** sheet was hence obtained.

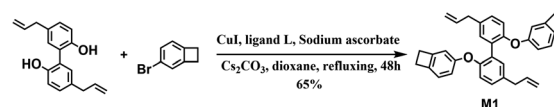
Preparation of the cured polymer films

The solution of **M1** (0.30 g) in mesitylene (3 mL) was heated under an atmosphere of N₂ at 200 °C for 1 h to obtain a pre-polymer. After cooling to room temperature, the pre-polymer solution was spin-coated onto the surface of a silicon wafer. The wafer was then put into a quartz tube furnace, and treated at 220 °C and 240 °C for 2 h, respectively. Thus, a cured **M1** film was obtained.

Results and discussion

Synthesis and characterization

Starting from magnolol, bio-based monomer **M1** was successfully synthesized in a moderated yield of 65% through a facile



Scheme 1 Procedure for the synthesis of **M1**.

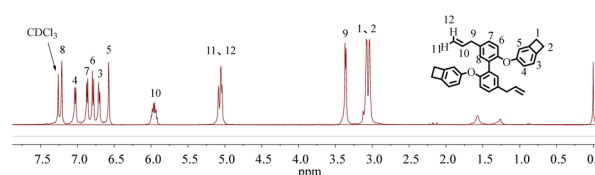


Fig. 1 ¹H NMR spectrum of **M1** in CDCl₃ at 400 MHz.

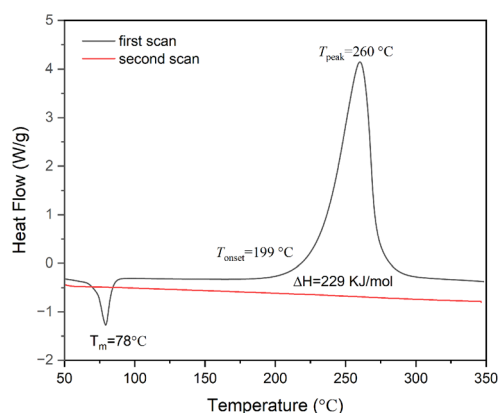
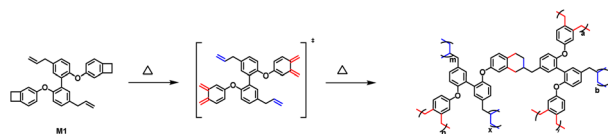
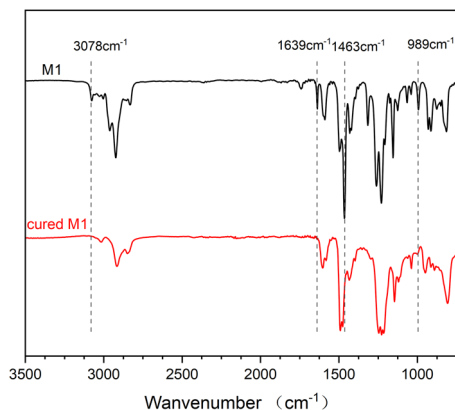


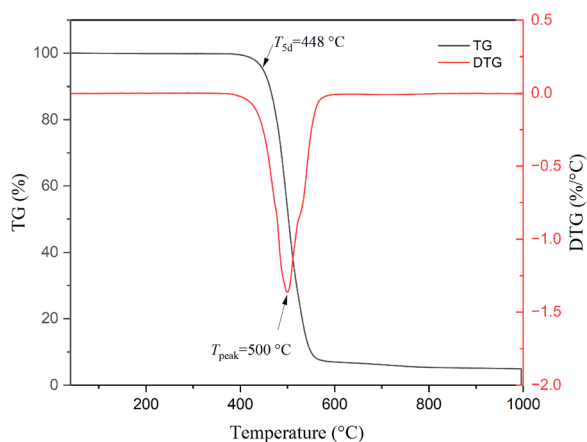
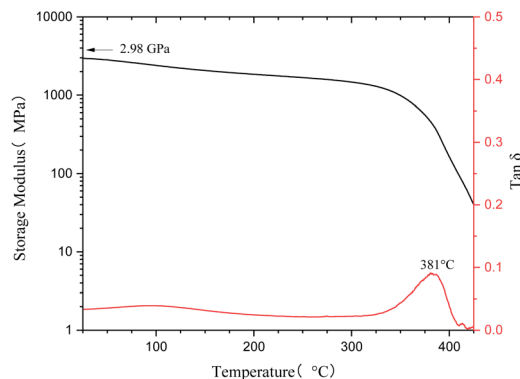
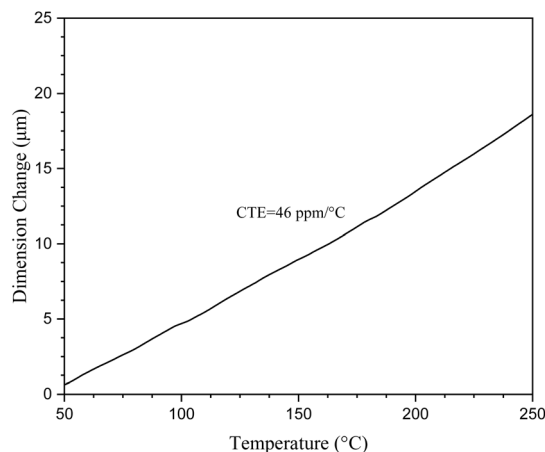
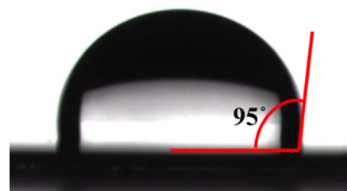
Fig. 2 DSC traces of **M1** at a heating rate of 10 °C min⁻¹ in N₂.



Scheme 2 Schematic curing mechanism of monomer **M1**.Fig. 3 FT-IR spectra of **M1** before and after curing.

one-step procedure, as shown in Scheme 1. Such a functionalized monomer with thermal cross-linkable BCB groups is easily soluble in common organic solvents such as toluene, chloroform, THF and acetone, implying its good processability.

The chemical structure of **M1** was characterized by ^1H NMR, ^{13}C NMR, HRMS-EI and elemental analysis. The ^1H NMR spectrum of **M1** is shown in Fig. 1. As seen in Fig. 1, the peaks in the range of 6.57 ~ 7.25 belong to the protons on the aromatic rings in the molecule. The characteristic peaks at 5.95, 5.06, and 3.36 ppm are assigned to the protons on the double-bond of propenyl groups. The peaks at 3.06 ppm are ascribed to the protons of the methylene group of BCB. The ^{13}C NMR spectrum (see Fig. S1 in ESI†) further provides information to confirm the structure of **M1**. Moreover, the FT-IR spectrum, HRMS-EI and elemental analysis data of the

Fig. 4 TGA curve of cured **M1** at a heating rate of 10 °C min⁻¹ in N₂.Fig. 5 DMA curves of cured **M1** at a heating rate of 5 °C min⁻¹ in N₂.Fig. 6 CTE curve of cured **M1** at a heating rate of 5 °C min⁻¹ in N₂.Fig. 7 A photo image of the static contact angle of water on the surface of the cured **M1** film.Table 1 Properties of cured **M1**

D_k	D_f	$T_{sd}/^\circ\text{C}$	$T_g/^\circ\text{C}$	CTE/ppm °C ⁻¹	Water uptake ^a
2.78	1.0×10^{-3}	448	381	46	0.50%

^a Measured after immersing the samples in boiling water for 96 h.

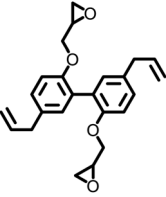
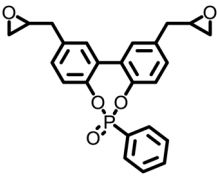
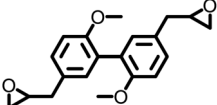
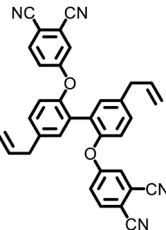
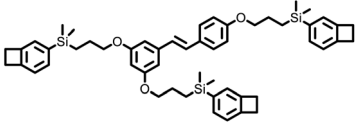
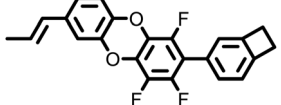
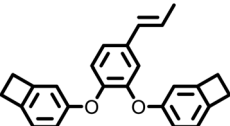
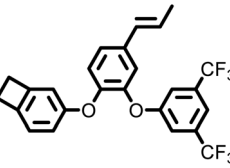
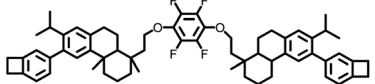
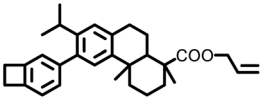
monomer (see Experimental section) are also consistent with the proposed structure.

Curing behavior of the monomer

After heating at high temperatures, monomer **M1** can be converted into a cross-linked polymer (cured **M1**). The thermal



Table 2 Comparison of the properties of cured M1

		T_g	T_{5d}	D_k	D_f	Frequency	References
Magnolol-based polymers		279	402	—	—	—	9
		—	337	—	—	—	8
		151	329	—	—	—	6
		>500	527.6	—	—	—	10
		—	431	2.68	8.4×10^{-3}	5 GHz	39
Bio-based BCB-containing resins		334	483	2.60	1.4×10^{-3}	10 GHz	33
		384	474	2.59	5.4×10^{-3}	5 GHz	19
		132	473	2.56	1.2×10^{-3}	5 GHz	19
		254	405	2.44	2.3×10^{-3}	15 MHz	37
A product from DOW chemicals		261	406	2.51	5.0×10^{-3}	0.1 ~ 18 MHz	38
	Cyclotene™ This work	293 381	446 448	2.70 2.78	8.0×10^{-3} 1.0×10^{-3}	1 MHz 10 GHz	46



crosslinking reaction of monomer **M1** was monitored by DSC, and the results are exhibited in Fig. 2. As shown in Fig. 2, **M1** displays a melting point of 78 °C and an onset curing temperature of 199 °C. The maximum exothermic peak temperature is observed at about 260 °C. At the second scan, no exothermic peak is observed, illustrating that monomer **M1** has cured completely. The curing of **M1** is related to the ring-open reaction of the BCB four-membered ring of the molecule. At high temperature, BCB groups have a tendency to form diradical or *o*-quinodimethane intermediates,³⁶ which further convert to the homopolymer through a self-polymerization reaction or change to the copolymers by the Diels–Alder reaction with the double bond-containing molecules or groups. To well understand the curing process of **M1**, a schematic curing mechanism is depicted in Scheme 2.

The curing reaction degree of **M1** was studied by FT-IR spectroscopy, and the results are shown in Fig. 3. As can be seen from Fig. 3, the characteristic peaks of BCB at 1463 cm^{−1} and 989 cm^{−1} disappear after curing, and the characteristic peaks of allyl groups at 1639 cm^{−1} and 3078 cm^{−1} also disappear, suggesting that the curing reaction has completed and the allyl groups have participated in the curing reaction.

Thermostability of cured **M1**

The thermostability of cured **M1** was explored by TGA, and the results are shown in Fig. 4. Under a N₂ atmosphere, cured **M1** exhibited a 5% weight loss temperature (*T*_{5d}) of 448 °C, such a *T*_{5d} is superior to that of magnolol-based epoxy,^{8,9} as well as better than those of most of the bio-based polymers.^{37–39} The high thermostability may be ascribed to the rigid aromatic structure of the monomer.

Dynamic mechanical properties of cured **M1** were studied by DMA, and the results are depicted in Fig. 5. Estimating the peak of tan δ gives a glass transition temperature (*T*_g) of 381 °C for cured **M1**. Such a high *T*_g implies the existence of a highly cross-linked network in cured **M1**. It can also be seen from Fig. 5 that cured **M1** has a high *E'* of 2.98 GPa at room temperature and a *E'* of over 1.4 GPa even at a temperature of 300 °C. These data also suggest there is a highly cross-linked network in cured **M1**.

Thermal dimensional stability is an important parameter for materials used in the microelectronics industry. In our case, the thermal dimensional stability of cured **M1** was evaluated by the coefficient of thermal expansion (CTE), which was measured by TMA. Fig. 6 depicts the CTE test results. As can be seen from Fig. 6, cured **M1** exhibits a CTE of 46 ppm °C^{−1} in the temperature range of 50 to 250 °C. This CTE of cured **M1** is lower than those of most of the low dielectric polymers, such as epoxy resins (72 ppm °C^{−1})⁴⁰ and PPOs (56 ppm °C^{−1}).⁴¹

Hydrophobicity

High hydrophobicity is very important for polymers applied in the microelectronics field because it protects the devices from deterioration by moisture.⁴² In this contribution, the hydrophobicity of cured **M1** was characterized by measuring the static water contact angle of water on the surface of the cured **M1** film coated on a silicon wafer. As shown in Fig. 7, the contact angle

of water on the surface of the cured **M1** film is 95°. Further, water uptake of cured **M1** was determined by immersing a cured resin sheet in boiling water for 96 h. The results indicate that cured **M1** displays a water uptake of 0.5%. These results suggest that cured **M1** possesses good hydrophobicity.

Dielectric properties

One of the most important usages for low dielectric materials is as encapsulation resins used in the electronics and microelectronics industries.⁴³ Thus, satisfactory low dielectric materials should possess a low dielectric constant (*D*_k) and low dielectric loss (*D*_f). In particular, low *D*_k and *D*_f are favorable for modern communication technology because they can solve the problems of signal delay and loss.^{34,44} *D*_k and *D*_f of cured **M1** were measured using a split post dielectric resonator method at a frequency of 10 GHz, and the results are listed in Table 1. As summarized in Table 1, cured **M1** displays a *D*_k of 2.78 with a *D*_f of 1.0 × 10^{−3} at a frequency of 10 GHz. The *D*_k is lower than those of many commonly used dielectric materials,^{28,41} especially, the *D*_f is lower than those of most commercial dielectric materials, such as polyimides (1.0 × 10^{−2}),²⁸ epoxy resins (2.0 × 10^{−2}),⁴⁰ and PPO (4.7 × 10^{−3}).⁴¹ Dielectric materials with ultra low *D*_f are necessary for the improvement of the signal transmission quality of high-frequency communication.⁴⁵ The low *D*_k and *D*_f can be attributed to the unique structure of **M1**. The rigidity and high torsional structure of **M1** can enhance the free volume of the polymer and reduce the packing degree of the molecular chains, which are helpful to achieve low *D*_k of the cured resins. The multiple thermo-cross-linkable groups endow the cured polymer with high crosslinking density, which is beneficial to limit the movement of the dipoles in the polymers. As a result, cured **M1** exhibits a low *D*_f.

Comprehensive properties of cured **M1**

A comparison of comprehensive properties of cured **M1** with magnolol-based polymers and some reported bio-based BCB-containing resins is summarized in Table 2. As can be seen from Table 2, cured **M1** exhibits good comprehensive properties, and it is also comparable to commercial products.⁴⁶

Conclusion

In summary, we have successfully synthesized a functional monomer with thermally cross-linkable benzocyclobutene groups from bio-based magnolol through a one-step Ullman–Ma reaction. The thermally cross-linked product of the monomer displays good comprehensive properties including a low *D*_k of 2.78 and low *D*_f of 1.0 × 10^{−3} at a frequency of 10 GHz, high *T*_{5d} of 448 °C, high *T*_g of 381 °C and low CTE of 46 ppm °C^{−1} in the temperature range of 50 to 250 °C. Such properties are comparable to those of magnolol-based polymers and the reported benzocyclobutene-containing polymers, suggesting the bio-based monomer reported in this contribution is a suitable precursor for encapsulation resins for application in the microelectronics industry.



Author contributions

Zhuoyi Yang: synthesis, investigation, data-collection, writing – original draft. Jing Sun: supervision, writing – review & editing. Qiang Fang: supervision, conceptualization, writing – review & editing.

Conflicts of interest

There are no conflicts to declare.

Acknowledgements

Financial support from the Strategic Priority Research Program of the Chinese Academy of Sciences (Grant No. XDB 0590100) and Natural Science Foundation of China (NSFC, No. 21975278, 22075311, and 22175195) Technology Commission of Shanghai Municipality (23ZR1476200) is gratefully acknowledged.

References

- 1 K. Bang, Y. Kim, B. Min, M. Na, Y. Rhee, J. Lee and K. Bae, *Arch. Pharmacol. Res.*, 2000, **23**, 46–49.
- 2 Y. Lee, Y. Lee, C. Lee, J. Jung, S. Han and J. Hong, *Pharmacol. Ther.*, 2011, **130**, 157–176.
- 3 A. Sarrica, N. Kirika, M. Romeo, M. Salmona and L. Diomedea, *Planta Med.*, 2018, **84**, 1151–1164.
- 4 J. Shen, K. Man, P. Huang, W. Chen, D. Chen, Y. Cheng, P. Liu, M. Chou and Y. Chen, *Molecules*, 2010, **15**, 6452–6465.
- 5 K. Watanabe, H. Watanabe, Y. Goto, M. Yamaguchi, N. Yamamoto and K. Hagino, *Planta Med.*, 1983, **49**, 103–108.
- 6 M. Bu, X. Zhang, T. Zhou and C. Lei, *Eur. Polym. J.*, 2022, **180**, 111595.
- 7 W. Guo, F. Liang, S. Chen, D. Zhang, W. Li, K. Qian, Y. Xu and B. Fei, *Polym. Degrad. Stab.*, 2022, **202**, 110002.
- 8 C. Ma, L. Qian and J. Li, *Polym. Degrad. Stab.*, 2021, **190**, 109630.
- 9 Y. Qi, Z. Weng, K. Zhang, J. Wang, S. Zhang, C. Liu and X. Jian, *Chem. Eng. J.*, 2020, **387**, 124115.
- 10 Z. Weng, L. Song, Y. Qi, J. Li, Q. Cao, C. Liu, S. Zhang, J. Wang and X. Jian, *Polymer*, 2021, **226**, 123814.
- 11 M. Dai, Y. Tao, L. Fang, C. Wang, J. Sun and Q. Fang, *ACS Sustain. Chem. Eng.*, 2020, **8**, 15013–15019.
- 12 S. Galli, A. Cimino, J. Ivy, C. Giacobbe, R. Arvapally, R. Vismara, S. Checchia, M. Rawshdeh, C. Cardenas, W. Yaseen, A. Maspero and M. Omary, *Adv. Funct. Mater.*, 2019, **29**, 1904707.
- 13 G. Maier, *Prog. Polym. Sci.*, 2001, **26**, 3–65.
- 14 D. Shamiryan, T. Abell, F. Iacopi and K. Maex, *Mater. Today*, 2004, **7**, 34–39.
- 15 M. Shi, G. Huang, J. Sun and Q. Fang, *Polym. Chem.*, 2023, **14**, 999–1006.
- 16 S. Shi, X. Liao, W. Tang, P. Song, F. Zou, Z. Fan, F. Guo and G. Li, *Adv. Eng. Mater.*, 2022, **24**, 2100874.
- 17 L. Wang, X. Liu, C. Liu, X. Zhou, C. Liu, M. Cheng, R. Wei and X. Liu, *Chem. Eng. J.*, 2020, **384**, 123231.
- 18 Y. Wang, Y. Tao, J. Zhou, J. Sun and Q. Fang, *ACS Sustain. Chem. Eng.*, 2018, **6**, 9277–9282.
- 19 F. Liu, Q. Fang and J. Sun, *ACS Appl. Polym. Mater.*, 2022, **4**, 7173–7181.
- 20 P. Dutta, B. Saikia, P. Alapati and K. Borah, *J. Electron. Mater.*, 2021, **50**, 1434–1443.
- 21 Z. Feng, X. Liu, W. Zhang, J. Zeng, J. Liu, B. Chen, J. Lin, L. Tan and L. Liang, *J. Mater. Sci.*, 2022, **57**, 1156–1173.
- 22 S. Wang, S. Ma, N. Li, S. Jie, Y. Luo and X. Gao, *Eur. Polym. J.*, 2023, **196**, 112302.
- 23 K. Li, *China Pat.*, CN116240733A, 2022.
- 24 W. Lin, T. Huang, J. You, Y. Xu, *World Pat.*, WO2022088239A1, 2022; W. Lin, T. Huang, J. You, Y. Xu, *China Pat.*, CN114478850A, 2022.
- 25 L. Peng, H. Bu, L. Bu, *China Pat.*, CN114958188A, 2022; L. Peng, H. Bu, L. Bu, *China Pat.*, CN114958188B, 2023.
- 26 R. Sun, P. Xu, J. Yu, S. Yu, S. Luo, *China Pat.*, CN115565717A, 2023; R. Sun, P. Xu, J. Yu, S. Yu, S. Luo, *World Pat.*, WO2024045159A1, 2024.
- 27 Y. Zhou, *China Pat.*, CN115583815A, 2022.
- 28 Y. Feng, J. Sun and Q. Fang, *ACS Appl. Polym. Mater.*, 2023, **5**, 4419–4426.
- 29 M. Huangfu, D. Shen, X. Zhi, Y. Zhang, Y. Jia, Y. An, X. Wei and J. Liu, *Nanomaterials*, 2021, **11**, 537.
- 30 F. Liu, J. Sun and Q. Fang, *ACS Appl. Polym. Mater.*, 2022, **4**, 842–848.
- 31 J. Wang, J. Zhou, K. Jin, L. Wang, J. Sun and Q. Fang, *Macromolecules*, 2017, **50**, 9394–9402.
- 32 P. Rae and D. Dattelbaum, *Polymer*, 2004, **45**, 7615–7625.
- 33 H. Zhang, J. Sun and Q. Fang, *Eur. Polym. J.*, 2022, **179**, 111527.
- 34 W. Volksen, R. Miller and G. Dubois, *Chem. Rev.*, 2010, **110**, 56–110.
- 35 J. Hou, J. Sun and Q. Fang, *Eur. Polym. J.*, 2022, **163**, 110943.
- 36 M. Marks, J. Erskine and D. Mccrery, *Macromolecules*, 1994, **27**, 4114–4126.
- 37 F. Fu, M. Shen, D. Wang, H. Liu, S. Shang, F. Hu, Z. Song and J. Song, *Biomacromolecules*, 2022, **23**, 2856–2866.
- 38 F. Fu, D. Wang, M. Shen, S. Shang, Z. Song and J. Song, *RSC Adv.*, 2019, **9**, 29788–29795.
- 39 G. Huang, L. Fang, C. Wang, M. Dai, J. Sun and Q. Fang, *Polym. Chem.*, 2021, **12**, 402–407.
- 40 X. Chen, J. Hou, Q. Gu, Q. Wang, J. Gao, J. Sun and Q. Fang, *Polymer*, 2020, **195**, 122443.
- 41 C. Chen, Z. Gu, Y. Tsai, R. Jeng and C. Lin, *Polymer*, 2018, **140**, 225–232.
- 42 H. Yuan, J. Xu and L. Xie, *Mater. Chem. Phys.*, 2011, **129**, 1195–1200.
- 43 X. Zhao and H. Liu, *Polym. Int.*, 2010, **59**, 597–606.
- 44 M. Li, J. Sun and Q. Fang, *Polym. Chem.*, 2021, **12**, 4501–4507.
- 45 Z. Hu, X. Liu, T. Ren, H. Saeed, Q. Wang, X. Cui, K. Huai, S. Huang, Y. Xia, K. Fu, J. Zhang and Y. Chen, *Polym. Eng. Sci.*, 2022, **42**, 677–687.
- 46 D. Burdeaux, P. Townsend, J. Carr and P. Garrou, *J. Electron. Mater.*, 1990, **19**, 1357–1364.

